Phase transition in an Aubry-André system with a rapidly oscillating magnetic field

Tridev Mishra,[*] Rajath Shashidhara,[†] Tapomoy Guha Sarkar,[‡] and Jayendra N. Bandyopadhyay[§]
Department of Physics, Birla Institute of Technology and Science, Pilani 333031, India
(Received 20 April 2016; revised manuscript received 22 September 2016; published 14 November 2016)

We investigate a variant of the Aubry-André-Harper (AAH) model corresponding to a bosonic optical lattice of ultracold atoms under an effective oscillatory magnetic field. In the limit of high-frequency oscillation, the system maybe approximated by an effective time-independent Hamiltonian. We have studied localization-delocalization transition exhibited by the effective Hamiltonian. The effective Hamiltonian is found to retain the tight-binding tridiagonal form in position space. In a striking contrast to the usual AAH model, this non-dual system shows an energy-dependent mobility edge—a feature which is usually reminiscent of Hamiltonians with beyond-nearest-neighbor hoppings in real space. Finally, we discuss possibilities of experimentally realizing this system in optical lattices.

DOI: 10.1103/PhysRevA.94.053612

I. INTRODUCTION

Ever since its proposal by Anderson [1], localization, and transitions between localized and extended states, have been studied in a variety of systems [2]. Extensive analysis has been undertaken to understand various aspects of metal-insulator transitions, localization as well as the existence of mobility edges in quasiperiodic or disordered one-dimensional (1D) lattices using scaling and renormalization techniques [3–10]. A system which has served as a rich prototype for such studies is the Hamiltonian, originally due to Harper [11], and investigated for phase transitions by Aubry and André [12].

An important feature of the Harper Hamiltonian is the existence of a metal-insulator transition [12] reminiscent of an Anderson transition. However, a notable difference is the absence of an energy-dependent mobility edge separating the localized and extended states, which is a distinguishing feature of the Anderson transition in three dimensions (3D). The Aubry-André-Harper (AAH) Hamiltonian exhibits a sharp, duality driven, transition at a unique critical value of the lattice modulation strength for all energies [13–16]. An ensuing trend in recent works has been to develop variations on the model which manifest a Anderson-transition-like mobility edge [17,18].

The quest is legitimized further by the substantial progress made by the cold atom community in reproducing complex condensed-matter phenomena including Anderson localization [19,20].

The experimental investigation of localization in 1D systems, especially of the incommensurate crystalline variety has witnessed a sustained interest ever since such lattices could be realized by using ultracold atoms in a bichromatic optical potential, or photonic quasicrystals [20–27]. These studies have ranged from direct experimental demonstration [20,22,28–31] to numerical calculations [23–25] with accompanying proposals for observing the appearance of localized phases and the metal to insulator or superfluid to Mott insulator transition (in the presence of interactions). Here, the control on the degree of commensurability has helped to identify the point of transition which, in the AAH model is the self-duality-induced critical point [27]. The Hofstadter variant and the AAH model in a two-dimensional (2D) optical lattice have also been successfully realized [32,33], in the context of simulating homogeneous magnetic fields in optical lattices. The effects of periodic driving on localization phenomena in 1D disordered systems as a possible means of weakening localization and arriving at extended or nonlocal states has shown encouraging results [34,35]. Similar pursuits in AAH systems with a view to analyzing diffusive transport behavior and wave-packet dynamics in the presence of driving have been promising in terms of appearance of delocalized states [36–38].

The technique of "shaking" of ultracold atoms in optical lattices has risen to prominence as a flexible means of generating new effective Hamiltonians which may replicate the effects of disorder, curvature, stresses and strains, and several other phenomena as synthetic gauge fields both Abelian or non-Abelian [21,39–41]. Some recent studies in driven cold atom setups have looked at induced resonant couplings between localized states, thereby making them extended [42] or at localization through incommensurate periodic kicks to an optical lattice [43]. In these models, the phase transition, instead of being driven by disorder, is a consequence of deliberate incommensurate periodicity. Demonstration of this behavior has also been sought in a phase-space analysis of the transition [44,45].

However, conspicuous by their absence have been works which look at the AAH model with a rapidly oscillating magnetic field, using the extensive tunability of cold atom setups. The existing study of AAH systems assumes the magnetic field to be static in time. If the magnetic field is periodic, then one may find a perturbative solution in the limit of high-frequency driving. We address this neglected aspect by employing a formalism based on Floquet analysis to obtain an approximate effective time-independent Hamiltonian for the system [46–51]. A pertinent enquiry about the effective system would be to look for a metal-to-insulator phase transition with an energy-dependent mobility edge.

In this work, we consider a high-frequency, sinusoidal effective magnetic field which couples minimally to the AAH

[*]tridev.mishra@pilani.bits-pilani.ac.in
[†]rajath.shashidhara@gmail.com
[‡]tapomoy1@gmail.com
[§]jnbandyo@gmail.com

Hamiltonian. The effective Hamiltonian is obtained for this system and its localization characteristics are compared with the usual self-dual AAH model in real and Fourier space. An energy-dependent mobility edge has already been studied in the context of an AAH Hamiltonian with an exponentially decaying strength of hopping parameters (beyond-nearest-neighbor coupling) [17]. We explore the possibility of a similar mobility edge in our physically motivated effective Hamiltonian with only nearest-neighbor hopping. The non-self-dual nature of our model is analyzed and some general features are investigated. In the discussion section, we attempt to reconcile our findings for the specific case with generic features of such non-dual models thereby putting the results in perspective. Finally, we discuss some possible experimental techniques that could be adapted to realize a version of the model presented here. Here, we highlight the difficulties involved in doing so and compare our model to some other driven cold atom AAH models in the literature.

II. FORMALISM

Recent successes in synthesizing tunable, possibly-time-dependent artificial gauge fields for systems of ultracold neutral atoms in optical lattices [52,53] has opened a gateway to the strong-field regime required for Hofstadter-like systems [54]. The system to be studied here may also be realized as an incommensurate superposition of two 1D optical lattices [27], with the laser beams for one of them undergoing a time-dependent frequency modulation. This shall be discussed in detail later, under Experimental Aspects.

We consider a tight-binding Hamiltonian with nearest-neighbor coupling that can be expressed as a time-dependent Aubry-André-Harper Hamiltonian of the form $H(t) = H_0 + V(t)$, where

$$\begin{aligned} H_0 &= \sum_n |n\rangle\langle n+1| + |n\rangle\langle n-1|, \\ V(t) &= V_0 \sum_n \cos[2\pi\alpha_0 n \cos(\omega t) + \theta]|n\rangle\langle n|. \end{aligned} \tag{1}$$

The summation here runs over all lattice sites. The time-dependent parameter $\alpha(t) = \alpha_0 \cos(\omega t)$ denotes the flux quanta per unit cell. An irrational value of α_0 renders the on-site potential quasiperiodic. The harmonic time dependence of $\alpha(t)$ owes its origin to a time-dependent magnetic field $\mathbf{B} = B_0 \cos(\omega t)\hat{\mathbf{z}}$. The other parameter θ is an arbitrary phase. The $|n\rangle$ are the Wannier states pinned to the lattice sites which are used as the basis for representing the Hamiltonian and V_0 denotes the strength of the on-site potential. The time dependence in the argument of the cosine modulation of the on-site potential is different from the usual time-dependent AAH models where it is in the overall magnitude of the on-site potential. The periodic time-dependent operator $V(t)$ can be expanded in a Fourier series as

$$V(t) = \widehat{V}_0 + \sum_{1\leqslant j<\infty} \widehat{V}_j e^{ij\omega t} + \sum_{1\leqslant j<\infty} \widehat{V}_{-j} e^{-ij\omega t}. \tag{2}$$

To obtain the effective time-independent Hamiltonian one writes the time evolution operator as

$$U(t_i, t_f) = e^{-i\hat{F}(t_f)} e^{-iH_{\text{eff}}(t_f - t_i)} e^{i\hat{F}(t_i)}, \tag{3}$$

where one introduces a time-dependent Hermitian operator $\hat{F}$. The idea is to push all the time dependence to the initial and final "kick" terms and render the main time evolution to be dictated by a time-independent Hamiltonian. The systematic formalism yields in the limit of large ω the following perturbative expansion for the effective time-independent Hamiltonian given by [50]

$$\begin{aligned} H_{\text{eff}} = {} & H_0 + \widehat{V}_0 + \frac{1}{\omega}\sum_{j=1}^{\infty}\frac{1}{j}[\widehat{V}_j, \widehat{V}_{-j}] \\ & + \frac{1}{2\omega^2}\sum_{j=1}^{\infty}\frac{1}{j^2}([[\widehat{V}_j, H_0], \widehat{V}_{-j}] + \text{H.c.}) + O(\omega^{-3}), \end{aligned} \tag{4}$$

where ω^{-1} is the small perturbation parameter, and the series is truncated at $O(\omega^{-2})$. To find the effective approximate Hamiltonian representing our system in the large-ω limit, one needs to compute the Fourier coefficients in Eq. (2). This is done by using the following commonly valid expansions [55]:

$$\begin{aligned} \cos(r\cos x) &= \mathcal{J}_0(r) + 2\sum_{p=1}^{\infty}(-1)^p \mathcal{J}_{2p}(r)\cos(2px), \\ \sin(r\cos x) &= 2\sum_{p=1}^{\infty}(-1)^{p-1}\mathcal{J}_{2p-1}(r)\cos[(2p-1)x], \end{aligned} \tag{5}$$

where $\mathcal{J}_n(r)$ are Bessel functions of order n. The Fourier coefficients of $V(t)$ may be obtained by inverting Eq. (2) by using these expansions. We obtain

$$\begin{aligned} \widehat{V}_j &= (-1)^{\frac{j}{2}} V_0 \cos\theta \sum_n \mathcal{J}_j(2\pi\alpha_0 n)|n\rangle\langle n|, \quad j = \pm 2,4,6,\ldots, \\ \widehat{V}_j &= (-1)^{\frac{j+1}{2}} V_0 \sin\theta \sum_n \mathcal{J}_j(2\pi\alpha_0 n)|n\rangle\langle n|, \quad j = \pm 1,3,5,\ldots, \\ \widehat{V}_0 &= V_0 \cos\theta \sum_n \mathcal{J}_0(2\pi\alpha_0 n)|n\rangle\langle n|. \end{aligned} \tag{6}$$

We find that $[\widehat{V}_j, \widehat{V}_{-j}] = 0$ owing to the symmetric nature of the Fourier coefficients (for real V). Therefore, the $O(\omega^{-1})$ correction to the effective Hamiltonian vanishes and the first nontrivial correction is at $O(\omega^{-2})$. The $O(\omega^{-2})$ term of the effective Hamiltonian would require the commutator bracket $[[\widehat{V}_j, H_0], \widehat{V}_{-j}]$, which on evaluation yields

$$[[\widehat{V}_j, H_0], \widehat{V}_{-j}] = \begin{cases} \sum_n -V_0^2 \cos^2\theta[(\mathcal{J}_j(2\pi\alpha_0(n+1)) - \mathcal{J}_j(2\pi\alpha_0 n))^2|n\rangle\langle n+1| \\ \quad +(\mathcal{J}_j(2\pi\alpha_0(n-1)) - \mathcal{J}_j(2\pi\alpha_0 n))^2|n\rangle\langle n-1|] & \text{if } j = \pm 2,4,6,\ldots \\ \sum_n -V_0^2 \sin^2\theta[(\mathcal{J}_j(2\pi\alpha_0(n+1)) - \mathcal{J}_j(2\pi\alpha_0 n))^2|n\rangle\langle n+1| \\ \quad +(\mathcal{J}_j(2\pi\alpha_0(n-1)) - \mathcal{J}_j(2\pi\alpha_0 n))^2|n\rangle\langle n-1|] & \text{if } j = \pm 1,3,5,\ldots. \end{cases} \tag{7}$$

By using the above expression in Eq. (4) we obtain the effective Hamiltonian, $H_{\rm eff}$, for our system. We find that, up to $O(\omega^{-2})$, the effective Hamiltonian yields a nearest-neighbor tight-binding model with a zeroth-order Bessel function modulating the site energies, and higher-order Bessel functions make their appearance in the hopping terms. There have been works which have looked at inhomogeneities in the hopping of the AAH model, arising not from driving but from the choice of next-nearest-neighbour hoppings in the corresponding 2D quantum Hall model [56–59]. However, these models consider situations where the off-diagonal modulations are quasiperiodic through incommensurate modifications of cosine kind of terms. In our case above, the incommensurability is embedded in higher-order Bessel functions, thereby variations in hopping strength are far more erratic and with signatures bordering on those of disorder. This is expected to have ramifications for both localized or extended behavior of the eigenstates. This is discussed in the next section and illustrated through localization phase plots.

III. RESULTS

The simple AAH model has a well-studied transition from a localized (insulating) to a delocalized (metallic) phase which occurs at a critical value $V_0 = 2$. To quantify the localization property we use the inverse participation ratio (IPR), which is defined as IPR $= \sum_{n=1}^{L} |a_n|^4 / (\sum_{n=1}^{L} |a_n|^2)^2$ where a_n are the expansion coefficients of the energy eigenstates in a local discrete-site basis and L is the number of lattice sites [60,61]. The IPR takes a value in the range 1 to $1/L$ with 1 indicating a perfectly localized state and $1/L$ for completely extended states. Figure 1(a) shows the transition in the real space IPR for the ground state of the AAH system with choice of irrational α_0

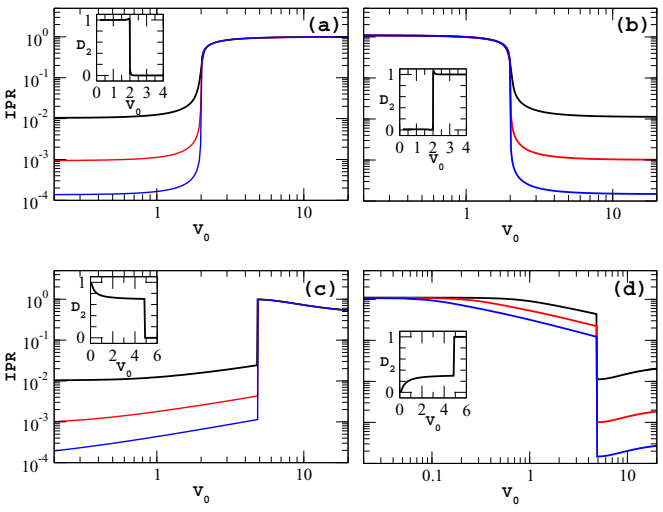

FIG. 1. (upper panel) The metal-to-insulator transition of the AAH Hamiltonian for the system's ground state. Plot (a) shows the IPR versus V_0 in real space for $L = 144$, 1597 and 10 946 (top to bottom). The inset shows the variation of D_2 with V_0 which also exhibits a transition. Plot (b) exhibits the mirror behavior in the dual space. (lower panel) The transition seen in the IPR versus V_0 curve for the $H_{\rm eff}$. Plots (c) and (d) are the real- and dual-space plots for the ground state with phase $\theta = 0$.

as inverse of the golden mean $(\sqrt{5}-1)/2$ and $L = 144$, 1597, and 10 946. The inset in this plot indicates variation in the magnitude of the quantity $|D_2|$ with V_0, where IPR $\propto L^{-D_2}$. For a given V_0, D_2 is obtained by fitting a linear regression line between ln IPR and ln L and thereby obtaining the slope. The regression fit is done by using several values of L, taken to be large Fibonacci numbers. In all the plots discussed here the transitions depicted are for some finite choice of system size and hence not exactly "step" changes but ramp up or down over some finite range of V_0 values. Furthermore, the references to such transitions as abrupt or occurring at a critical value have to be interpreted within such numerical constraints. D_2 values shows an abrupt transition from 1 to 0 at the critical value irrespective of lattice size. This establishes the transition to be a integral feature of the model even in the thermodynamic limit of infinite lattice size and the critical point is protected in this limit. To switch to states in the Fourier domain, i.e., $|m\rangle$ from the position space kets $|n\rangle$, we use the transformation

$$|m\rangle = \frac{1}{\sqrt{L}} \sum_{n} \exp(-i2\pi m\alpha_0 n)|n\rangle. \tag{8}$$

This enables one to write the AAH Hamiltonian in Fourier space and compute the IPR in this space. Figure 1(b) shows the transition in Fourier space for a set of parameters identical to those in Fig. 1(a). Here again, the characteristic transition occurs at the critical point $V_0 = 2$ and the curves in Fig. 1(a) are a mirror reflection of the curves in Fig. 1(b) about $V_0 = 2$. This is due to the exactly-self-dual nature of the AAH Hamiltonian. Thus, an extended regime in real space implies a localized one in Fourier space and vice versa. The inset for D_2 in Fourier space accordingly mirrors its real-space counterpart.

In the case of our effective model, the IPR for the ground state exhibits a similar trend, as shown in Fig. 1(c). The transition in this case for this state occurs at a new critical value $V_0 \approx 4.6$, all parameters being kept the same as in former plots. Another distinguishing feature of this transition for the driven case is the manner in which the IPR values approach the critical value and depart from it, relative to the behavior in the standard AAH model. In the extended regime, instead of the perfectly flat value of IPR ≈ 0, a slow positive gradient is observed, indicating weak localization that progressively gets stronger until a sharp surge occurs at the critical point. Even beyond the transition there is a fall in the IPR due to the still imperfect nature of the localization. This unique behavior can be partially attributed to the non-self-dual nature of the effective Hamiltonian which shall be discussed later. D_2, in the inset, continues to retain its scale-invariant attributes and manifests the imprint of the transition. The difference from the simple AAH model lies in the fall in its value from 1 to a lower plateau before the transition. An indication of the existence of a parameter regime where the state is neither purely localized nor extended but a sort of composite, i.e., critical and possibly multifractal. This is due to the unusual behavior of the wave function in the case of α_0 being a Liouville irrational number, whereby, for some lattice modulations, no finite localization length may be found over which the state could be said to appreciably decay [15,16]. Figure 1(d), which shows the Fourier-space IPR for our model exhibits reciprocal behavior of the kind seen in the simple AAH model but

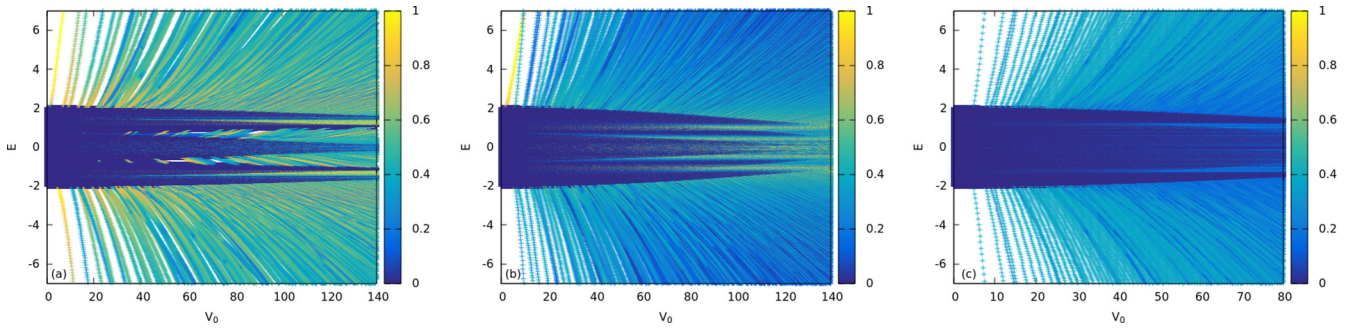

FIG. 2. The localization phase diagram with IPR in the (E, V_0) phase plane, for lattice size $L = 4181$ and three values of the variable θ: (a) $\theta = 0$, (b) $\theta = \pi/4$, (c) $\theta = \pi/2$.

with the major difference that Figs. 1(c) and 1(d) are not mirror reflected about the same critical value. This deviation is expected on grounds of the non-self-dual nature of our system's Hamiltonian. In Fourier space, D_2 analogously is not an exact mirror image of its real-space version but all other qualitative characteristics remain the same. There are features in the driven system's Fourier-space IPR which stand in contrast to the AAH model, as seen in Figs. 1(b) and 1(d). Most notably, the driven model shows a discrimination between the different lengths because the curves in Fig. 1(d) transition from localized to extended regimes at different rates. This is not the case in the ordinary AAH model, where all lengths transition together, as seen in Fig. 1(b). This difference is an indicator of non-nearest-neighbor couplings in our dual-space effective Hamiltonian and the accompanying anomalous behavior of the wave functions in a certain parameter range.

To understand how the properties of the transition are related to the normal modes of the effective driven system, we look at the localization phase diagram, i.e., the variation of IPR with V_0 and the low-energy region of the spectrum at each V_0 . Figure 2 shows the IPR in the V_0-E plane. We consider three such plots for values of the phase, $\theta = 0$, $\theta = \pi/4$, and $\theta = \pi/2$ in Eq. (1) and lattice size $L = 4181$. The nature of the variation of IPR reveals a sharp energy-dependent mobility edge for our model. The portion of the energy spectrum for which the IPR variation has been illustrated is chosen to clearly indicate the appearance of localized states. The choice of values for the phase is intended to isolate and compare the relative effects of the modified onsite term and the site-dependent hopping terms. In all three plots the sector corresponding to low-V_0 values and near to $E = 0$ shows a dense region of extended states which [see Eq. (1)], reflects the bare hopping structure.

The features in the these phase diagrams owe their origin to the relative dominance of different terms in the driven effective Hamiltonian for a given θ. The anisotropy of the zero-order Bessel modulated on-site energy adds impurity or disorder-like effects on top of the inherent quasiperiodicity of the model. The falloff of this on-site energy with lattice sites diminishes the actual system size to a reduced one. The modified hopping strengths are also site dependent and vary in an oscillatory manner, with a damping with increasing site index. When the onsite potential damps out, the hopping terms from H_0 survive. This is expected to contribute to an increase in the IPR as the behavior tends to one of a lattice with disorder. These factors collectively influence the spectral spread and density along with the localized-delocalized behavior of the various eigenstates.

Figure 2(a), for $\theta = 0$, depicts the appearance of quasilocalized states (yellow fringes) at the boundaries of the extended (deep blue) region. As V_0 increases, the dense region of extended states near $E = 0$ begins to manifest traces of localization in IPR values, introducing the mobility edges. This can be noted from the bifurcations of the phase boundary that begin to show up with increasing V_0 with localized eigenstates piercing into portions of the spectrum which at lower V_0 were dominated by extended states. For higher energy the IPR values vary primarily between critical and extended behavior. This is notably absent in the plots for $\theta = \pi/4$ and $\theta = \pi/2$ where critical behavior is hardly observed, and that too in a very narrow region around the phase boundary. The wider gapping in the eigenvalues as compared with the other two cases can be accorded to the overall stronger influence of the on-site term as compared to the hoppings.

Figure 2(b), for $\theta = \pi/4$, includes the effects of all the terms of the effective Hamiltonian. The appearance of localized states around $E = 0$ takes place as before. However, there is a notable lack of appearance of well-localized states in the higher-energy regions as compared with Fig. 2(a). This indicates a closer competition between the on-site and hopping terms of the driven model. The significant localization effects, hence mobility edges, appear distinctly in a band around $E = 0$ and that too at higher V_0. This may be accounted for by the fact that, for $\theta = \pi/4$, both the sine and cosine modulations are present in the modified hopping [see Eq. (7)], unlike the previous $\theta = 0$ case. Apart from contributing to the predominance of extended states in most of the spectrum, this more influential hopping part also makes the spectrum relatively less gapped.

Figure 2(c), for $\theta = \pi/2$ has been specifically shown to illustrate how the hopping terms in the driven AAH model behave in the absence of any on-site term. For this choice of θ the $\widehat{V_0}$ in Eq. (6) goes to zero. As expected in the presence of just the hopping, the IPR values show an extended behavior everywhere in the phase plot. However, one can still note a phase boundary differentiating the region of the purely extended states from somewhat less extended ones. The appearance and nature of the bifurcations in the boundary of this dense part of the phase plot with changing V_0 indicates the qualitative effects of the inhomogeneities in the hopping

terms. Looking at Figs. 2(a)–2(c) it is clear that the role of the modulated onsite has the effect of enhancing the localization of states as well as creating a sharper mobility edge.

This indicates that the driven model shows a strong sensitivity to the phase θ in terms of the localization behavior and the appearance of mobility edges. The number of these edges, as can be seen, is more for the $\theta = \pi/4$ case and is almost absent in the phase plot for $\theta = \pi/2$. A recent work [62] looks at a topological classification of AAH models with cosine-modulated hoppings which differ by a phase factor from the onsite modulation. This helps to realize topologically distinct families of AAH Hamiltonians with the possibility of topological phase transitions between the different classes via a modification of the lattice modulations. Similar behavior would be interesting to study in our driven context.

IV. DISCUSSION

To qualitatively analyze some of our results we consider a simplified model comprising of a trivial constant hopping term and an on-site potential T which is aperiodic or quasiperiodic. The Schrödinger equation is given by

$$a_{n+1} + a_{n-1} + \Lambda T(\alpha_0 n + \phi) a_n = E a_n, \tag{9}$$

where Λ is the strength of on-site energy and E are the energy eigenvalues. One can go to the dual space for the above system by defining an expansion, as follows:

$$a_n = \frac{e^{ikn}}{\sqrt{L}} \sum_m \tilde{a}_m e^{im(\alpha_0 n + \phi)}, \tag{10}$$

where the $\tilde{a}_m$ are the dual-space amplitudes, and k is a wave vector from the Bloch wave expansion ansatz. This allows T to be expressed as

$$T(\alpha_0 n + \phi) = \frac{1}{\sqrt{L}} \sum_{\acute{m}} \mathcal{T}_{\acute{m}} e^{i\acute{m}(\alpha_0 n + \phi)}. \tag{11}$$

Equations (10) and (11) yield an on-site term in the dual space from the the hopping terms of Eq. (9) as

$$a_{n-1} + a_{n+1} = \frac{e^{ikn}}{\sqrt{L}} \sum_m \tilde{a}_m e^{im(\alpha_0 n + \phi)} \cos(\alpha_0 m + k), \tag{12}$$

with a cosine modulation of the on-site energy (as seen in the Aubry-André model). Interestingly, the real-space on-site energy term transforms as

$$\Lambda T(\alpha_0 n + \phi) a_n = \frac{\Lambda e^{ikn}}{L} \sum_{\acute{m}} \sum_m \mathcal{T}_{\acute{m}} \tilde{a}_m e^{i(m+\acute{m})(\alpha_0 n + \phi)}. \tag{13}$$

The right-hand side (RHS) can be slightly rearranged to give

$$\frac{\Lambda e^{ikn}}{L} \sum_{\acute{m} \neq \pm 1} \sum_m \mathcal{T}_{\acute{m}} \tilde{a}_{m+\acute{m}} e^{im(\alpha_0 n + \phi)} + \frac{\Lambda e^{ikn}}{L} \sum_m (\mathcal{T}_1 \tilde{a}_{m-1} + \mathcal{T}_{-1} \tilde{a}_{m+1}) e^{im(\alpha_0 n + \phi)}. \tag{14}$$

In the above form, the second term clearly indicates the apparent nearest-neighbor hopping terms in the dual-space whose strength is modulated by the Fourier components of T. It is the first term in the above expression which explicitly breaks the exact duality. The form of $\mathcal{T}_{\acute{m}}$ determines the extent to which different m values in the dual space are coupled. It is well known that, for decaying oscillatory functions such as sinc and the Bessel function of the zeroth order, $\mathcal{T}_{\acute{m}}$ is a rectangular function, with possibly a $\acute{m}$-dependent modulation, symmetric about the origin. Thus, in our case, we expect a truncation effect in dual space which restricts the range of couplings. This deviation from exact duality is expected to have some impact on the probability of an "analytic accident" along the lines of Ref. [12]. The appearance of localized states (real eigenfunctions) happens when there are superpositions of counterpropagating plane waves with wave vectors of near-commensurate magnitude. This would mean, in our model, some harmonics from the expansion of T shall scatter the wave with wave vector k by an amount commensurate with $2n\pi$. This has to be considered together with the fact that, for a rational approximation of α_0 as a ratio of two large successive Fibonacci numbers, the true momentum (Fourier) space eigenvalues κ are related to m as $\kappa = m F_{i-1} \mathrm{mod} F_i$, where F_{i-1} and F_i are successive Fibonacci numbers [5,44]. Thus, what appear to be close neighbors in m could possibly be well separated in the actual wave-vector space. Furthermore, the range of m values that shall remain coupled in the dual space will be dictated by the extent of T in the real lattice, for example, the first zero in the Bessel function. The set of m which conspires with a given k value to yield a localized state shall be dictated by V_0 and $E(k)$. This explains the energy-dependent mobility edge in Fig. 2.

In the dual space, where k acts as a phase [see Eq. (12)], a state localized at few m values could be shifted by large amounts for a small change in k. This allows for the interpretation that a small change in ϕ could in effect cause a state localized around some lattice site to localize about a far-off site. In terms of symmetry, the absence of translational invariance in Euclidean space of quasiperiodic structures with two incommensurate periodicities can be restored in an extended space by using the ϕ dimension [63,64]. This effect of ϕ on localization properties leads to the differences between the three plots in Fig. 2.

V. EXPERIMENTAL ASPECTS

The experimental realization of our system may be achieved in several different ways, with ease and feasibility of implementation being the guiding criteria in the choice of method. We will explore two options here, from recent literature, which are promising. One way is to begin with a 2D optical lattice and then proceed in the manner described in some recent realizations of the Harper-Hofstadter Hamiltonian [32,33]. The notion of simulating a synthetic magnetic field by means of generating effective flux per plaquette of the lattice is a generic feature. However, the true appeal of these methods compared to others for generating artificial magnetic fields for ultracold neutral alkali-metal atoms in optical lattices, is the absence of coupling between different hyperfine states of the atoms. It is possible therefore to proceed with a single internal state and far-detuned lasers to achieve homogeneous magnetic fields by a laser-assisted hopping process. A pair of far-detuned Raman lasers is employed, while tunneling in a particular direction is obstructed by means of a gradient or ramp in the site

energies using gravity or magnetic fields, to restore resonant tunneling between sites. The AAH Hamiltonian is obtained in a time-independent effective way by averaging over the high-frequency terms and the hopping energy is modified by a complex position-dependent phase.

We suggest using Raman lasers of frequencies close to those of the optical lattice lasers, as prescribed by the authors, and to use the tunability of the flux per plaquette α_0 offered by such choice, to set it to an irrational value by adjusting the angle between the Raman beams. Introducing the time dependence is admittedly tricky. This is due to the fact that the static Harper Hamiltonian in the above technique is itself achieved by time averaging and we need it to have a further residual time dependence. For this one would have to vary α_0 periodically by say, modifying the angle between the Raman lasers periodically with time together with simultaneous time modulations of the detunings and the gradients in a fashion that the overall effect is of a periodic change that is of a rate slower than the oscillations to be averaged over while resonant tunneling occurs, but fast enough to remain detuned from the energy gap between the ground and excited Bloch bands of the trapped atoms in the lattice potential. This yields a timescale which survives the first averaging and gives one a time-dependent AAH Hamiltonian effectively being driven by an oscillating magnetic field. There are some obstacles to be overcome here such as arranging the time-dependent detunings and the angular variation of the Raman lasers so as to vary α_0 sinusoidally as a function of time effectively, since there is a good chance of getting high-frequency noisy components that have to be averaged over. Another issue is that the scheme does not realize the simple Landau gauge for a magnetic field. We use this gauge in our analysis but the results, essentially the nature and existence of the Metal-insulator transition, are independent of any such choice through the gauge freedom embodied in the choice of θ in the AAH Hamiltonian [12]. The analysis then would be modified only up to a gauge transformation. It would indeed be interesting if the method could be modified to include the Landau gauge.

On account of the multiple time-dependent modulations in the realization just discussed, heating and spontaneous photonic emission processes are a legitimate source of concern. We would like to outline another approach by using a quasiperiodic 1D optical lattice which may have better characteristics as regards dissipative processes. Here we suggest using the bichromatic 1D optical lattice realization of the AAH model as described in Ref. [27] and suitably modifying it to implement our model. Essentially, a bichromatic optical lattice setup is one with a pair of superposed standing waves wherein one provides the tight-binding structure to the Hamiltonian and the other, a weak secondary perturbing potential which, through adjustable noncommensurability of its wavelength with that of the first, offers a quasiperiodic or pseudorandom potential for the ultracold gas of atoms even to the extent of mimicking quasidisorder in the lattice [20]. The two standing waves have wavelengths in the ratio of two consecutive Fibonacci numbers. This helps to realize a workable notion of incommensurability in a finite lattice system by tending the value of the α_0 to near the inverse of the golden mean. As suggested in Ref. [27], this is the key requirement for the observation of a transition from extended to localized states, i.e., to keep a large number of lattice sites in a single period of the on-site potential for finite systems.

The next step is to systematically introduce the driving. This is done by introducing a time dependence in the ratio of the wavelengths of the two standing-wave lattices. More precisely, to do this we suggest generating the two standing waves by using beam splitting and retroreflection by mirrors. If now the reflecting mirror corresponding to the primary tight-binding lattice is shaken according to a protocol which mimics a sinusoidal drive say, by mounting it on a piezoelectric motor, it should be in principle possible to generate a sinusoidal time dependence in the irrational flux term. It would be preferable to use actuators that move the mirrors so as to produce acceleration effects on the lattice such that one may achieve time-dependent Doppler shifts in the frequency and hence wavelengths of the stationary waves (where one averages over the fast oscillations in the amplitudes to get the hopping terms) which could be controlled in a sinusoidal fashion. This may be technically demanding under the present capabilities of shaking in optical lattice systems but is definitely worth exploring as a powerful instrument for studying effective Hamiltonians in a new time-dependent regime.

In the two approaches highlighted above, the respective works [32] and [27] provide a clear map between the parameters of the simulated model and the experimental parameters such as laser intensities, recoil energies of the trapped neutral atoms, and the energy gap between the ground state and lowest-excited Bloch band in the lattice. This mapping translates readily to the formalism of calculating the effective Hamiltonian. For instance, in the case of the bichromatic construction the mapping of the continuous optical potential to a tight-binding picture has been carried out in Ref. [27] by using a set of local Wannier basis states. As per this construction our time-dependent model, see Eq. (1) would have V_0 be a ratio of product of the height of the weak perturbing lattice with the time-dependent ratio of the wavelengths of the two standing waves and an integral term, to the hopping element of the primary optical lattice. The term α_0 is just the ratio of the wavelengths of the two standing waves, made time dependent by shaking, which are two consecutive Fibonacci numbers. From the expressions in Eqs. (6) and (7) it can be readily seen how the experimental parameters enter into the modified on-site and nearest-neighbour hopping energy terms of the high-frequency effective static Hamiltonian for the driven system.

Thus the relation between parameters of the setup and the derived model Hamiltonian can be traced in a straightforward manner. It is true that this manner of constructing the system will make the strength of the on-site modulation (or its ratio with the hopping energy) also a sinusoidal function of time but this is not expected to alter the system's features studied here in any significant way. We propose studying this more general form of time dependence, with the strength of the on-site to off-site energy also taken to be a function of time alongside the periodicity in α_0, as a future line of work.

Briefly, we would like to survey how our work contrasts with other early and recent work, which has emphasized periodic driving through additional potentials [42] and shaking [21] in AAH systems. In Ref. [21], shaking introduces a time-dependent phase in the cosine term of the on-site energy.

This phase is separate from the incommensurate position dependence. The effect is a renormalization of the hopping energy so as to make it a function of the driving amplitude. This enables one to tune across the metal-insulator transition by varying the amplitude of the driving. Whereas in our system the driving is provided through an oscillatory effective magnetic field which manifests itself through the periodicity in α_0, and hence is present in the incommensurate position-dependent term.

This is again different from Ref. [42], which employs a driving that is a weak space quasiperiodic and time periodic perturbation onto the AAH system modeled as a quasiperiodic optical lattice. Here, the driving is a weak perturbation to the original AAH Hamiltonian. In our case, however, the manner in which the AAH model is driven is nonperturbative by its very nature. An oscillating magnetic field, even of small amplitude, is in no way a weak perturbation and cannot be treated as such; it has to be looked upon in the Floquet picture of periodic time-dependent Hamiltonians. The high-frequency nature of the driving permits a Floquet theoretic treatment of a slightly analytical variety through the high frequency expansion available for the Floquet Hamiltonian. Only here, in the parameter $1/\omega$, is one allowed to use a perturbative treatment. This is formally different from Ref. [42] in that our modifications significantly alter the AAH model for which there is limited analytical footing in the high-frequency regime. It would do well to regard the newly obtained static effective Hamiltonian as an independent system in its own right, with features that are not to be expected in the undriven or weakly driven AAH models. This in fact merits looking into, because it would not be unjustified to anticipate exotic modifications to the traditional AAH metal-insulator transition under these circumstances.

Also worth noting are the differences between the model in Ref. [42] and our system from a reciprocal-space point of view. While our model is also non-self-dual it has an exact 1D structure with couplings that are beyond nearest neighbor. In Ref. [42], the dual Hamiltonian is not exactly 1D and the extended states appear due to resonant couplings of localized states that are driving induced. This differs considerably from the mechanism (discussed in the previous section) that causes localization-delocalization behavior in our driven system. In fact, the non-self-duality of our model sets it apart even from undriven variations on the AAH model (with mobility edges) which are self-dual by construction [17,18], irrespective of the real-space couplings being nearest neighbor or beyond it.

VI. CONCLUSION

In this work we have studied the Aubry-André-Harper problem with an oscillatory magnetic field in the promising cold atom-optical lattice scenario. The problem is significantly simplified by going into an effective Hamiltonian which approximately represents the system in the limit of high-frequency magnetic field. We find that this effective Hamiltonian is non-self-dual, and although it exhibits a metal-insulator transition, it differs from the classic Aubry-André model in the emergence of an energy-dependent mobility edge. The nearest-neighbor coupling form of the effective Hamiltonian yields this feature which is commonly observed in disordered 3D systems or Aubry-André-like models with hoppings extending beyond nearest neighbor.

ACKNOWLEDGMENTS

T.M. would like to acknowledge Takashi Oka and Alessio Celi for valuable discussions on various theoretical and experimental aspects of the problem.

[1] P. W. Anderson, Phys. Rev. **109**, 1492 (1958).
[2] F. Evers and A. D. Mirlin, Rev. Mod. Phys. **80**, 1355 (2008).
[3] D. R. Grempel, S. Fishman, and R. E. Prange, Phys. Rev. Lett. **49**, 833 (1982).
[4] S. Ostlund, R. Pandit, D. Rand, H. J. Schellnhuber, and E. D. Siggia, Phys. Rev. Lett. **50**, 1873 (1983).
[5] M. Kohmoto, Phys. Rev. Lett. **51**, 1198 (1983).
[6] H. Hiramoto and M. Kohmoto, Phys. Rev. Lett. **62**, 2714 (1989).
[7] D. J. Thouless, Phys. Rev. Lett. **61**, 2141 (1988).
[8] S. Das Sarma, S. He, and X. C. Xie, Phys. Rev. Lett. **61**, 2144 (1988).
[9] S. Das Sarma, S. He, and X. C. Xie, Phys. Rev. B **41**, 5544 (1990).
[10] Y. Hashimoto, K. Niizeki and Y. Okabe, J. Phys. A: Math. Gen. **25**, 5211 (1992).
[11] P. G. Harper, Proc. Phys. Soc., London, Sect. A **68**, 879 (1955).
[12] S. Aubry and G. André, in *Group Theoretical Methods in Physics*, Annals of the Israel Physical Society, edited by L. Horwitz and Y. Neéman (American Institute of Physics, New York, 1980), Vol. 3.
[13] S. Ya. Jitomirskaya, Ann. Math. **150**, 1159 (1999).
[14] J. Bellissard and B. Simon, J. Funct. Anal. **48**, 408 (1982).
[15] B. Simon, Adv. Appl. Math. **3**, 463 (1982).
[16] J. E. Avron and B. Simon, Ann. Phys. (NY) **110**, 85 (1978).
[17] J. Biddle, B. Wang, D. J. Priour, Jr., and S. Das Sarma, Phys. Rev. A **80**, 021603(R) (2009); J. Biddle and S. Das Sarma, Phys. Rev. Lett. **104**, 070601 (2010); J. Biddle, D. J. Priour, Jr., B. Wang, and S. Das Sarma, Phys. Rev. B **83**, 075105 (2011).
[18] S. Ganeshan, J. H. Pixley, and S. Das Sarma, Phys. Rev. Lett. **114**, 146601 (2015).
[19] J. Billy *et al.*, Nature (London) **453**, 891 (2008).
[20] G. Roati *et al.*, Nature (London) **453**, 895 (2008).
[21] K. Drese and M. Holthaus, Phys. Rev. Lett. **78**, 2932 (1997).
[22] Y. Lahini, R. Pugatch, F. Pozzi, M. Sorel, R. Morandotti, N. Davidson, and Y. Silberberg, Phys. Rev. Lett. **103**, 013901 (2009).
[23] G. Roux, T. Barthel, I. P. McCulloch, C. Kollath, U. Schollwöck, and T. Giamarchi, Phys. Rev. A **78**, 023628 (2008).
[24] R. Roth and K. Burnett, Phys. Rev. A **68**, 023604 (2003).
[25] J. E. Lye, L. Fallani, C. Fort, V. Guarrera, M. Modugno, D. S. Wiersma, and M. Inguscio, Phys. Rev. A **75**, 061603(R) (2007).

[26] R. B. Diener, G. A. Georgakis, J. Zhong, M. Raizen, and Q. Niu, Phys. Rev. A **64**, 033416 (2001).
[27] M. Modungo, New J. Phys. **11**, 033023 (2009).
[28] B. Damski, J. Zakrzewski, L. Santos, P. Zoller, and M. Lewenstein, Phys. Rev. Lett. **91**, 080403 (2003).
[29] V. Guarrera, L. Fallani, J. E. Lye, C. Fort and M. Inguscio, New J. Phys. **9**, 107 (2007).
[30] G. Ritt, C. Geckeler, T. Salger, G. Cennini, and M. Weitz, Phys. Rev. A **74**, 063622 (2006).
[31] L. Fallani, J. E. Lye, V. Guarrera, C. Fort, and M. Inguscio, Phys. Rev. Lett. **98**, 130404 (2007).
[32] H. Miyake, G. A. Siviloglou, C. J. Kennedy, W. C. Burton, and W. Ketterle, Phys. Rev. Lett. **111**, 185302 (2013).
[33] M. Aidelsburger, M. Atala, M. Lohse, J. T. Barreiro, B. Paredes, and I. Bloch, Phys. Rev. Lett. **111**, 185301 (2013).
[34] H. Yamada and K. S. Ikeda, Phys. Rev. E **59**, 5214 (1999).
[35] D. F. Martinez and R. A. Molina, Phys. Rev. B **73**, 073104 (2006).
[36] R. Lima and D. Shepelyansky, Phys. Rev. Lett. **67**, 1377 (1991).
[37] L. Hufnagel, M. Weiss, A. Iomin, R. Ketzmerick, S. Fishman, and T. Geisel, Phys. Rev. B **62**, 15348 (2000).
[38] A. R. Kolovsky and G. Mantica, Phys. Rev. B **86**, 054306 (2012).
[39] E. Arimondo, D. Ciampini, A. Eckardt, M. Holthaus, and O. Morschand, in *Advances in Atomic, Molecular, and Optical Physics*, edited by P. Berman, E. Arimondo, and L. Chun (Academic Press, 2012), Vol. 61, Chap. 10, pp. 515–547.
[40] P. Hauke, O. Tieleman, A. Celi, C. Olschlager, J. Simonet, J. Struck, M. Weinberg, P. Windpassinger, K. Sengstock, M. Lewenstein, and A. Eckardt, Phys. Rev. Lett. **109**, 145301 (2012).
[41] T. Mishra, T. G. Sarkar, and J. N. Bandyopadhyay, Eur. Phys. J. B **88**, 231 (2015).
[42] L. Morales-Molina, E. Doerner, C. Danieli, and S. Flach, Phys. Rev. A **90**, 043630 (2014).
[43] P. Qin, C. Yin, and S. Chen, Phys. Rev. B **90**, 054303 (2014).
[44] Ch. Aulbach *et al.*, New J. Phys. **6**, 70 (2004).
[45] G.-L. Ingold, A. Wobst, Ch. Aulbach, and P. Hänggi, Eur. Phys. J. B **30**, 175 (2002); A. Wobst, G.-L. Ingold, P. Hänggi, and D. Weinmann, Phys. Rev. B **68**, 085103 (2003).
[46] T. P. Grozdanov and M. J. Rakovic, Phys. Rev. A **38**, 1739 (1988).
[47] S. Rahav, I. Gilary, and S. Fishman, Phys. Rev. A **68**, 013820 (2003).
[48] M. M. Maricq, Phys. Rev. B **25**, 6622 (1982).
[49] P. Avan, C. Cohen-Tannoudji, J. Dupont-Roc, and C. Fabre, J. Phys. (Paris) **37**, 993 (1976).
[50] N. Goldman and J. Dalibard, Phys. Rev. X **4**, 031027 (2014).
[51] M. Bukov, L. D'Alessio, and A. Polkovnikov, Adv. Phys. **64**, 139 (2015).
[52] J. Struck, C. Ölschläger, M. Weinberg, P. Hauke, J. Simonet, A. Eckardt, M. Lewenstein, K. Sengstock, and P. Windpassinger, Phys. Rev. Lett. **108**, 225304 (2012).
[53] Y. J. Lin, R. L. Compton, A. R. Perry, W. D. Phillips, J. V. Porto, and I. B. Spielman, Phys. Rev. Lett. **102**, 130401 (2009); Y. J. Lin, R. L. Compton, K. Jiménez-Garciá, J. V. Porto, and I. B. Spielman, Nature (London) **462**, 628 (2009).
[54] D. R. Hofstadter, Phys. Rev. B **14**, 2239 (1976).
[55] M. Abramowitz and I. A. Stegun, *Handbook of Mathematical Functions with Formulas, Graphs, and Mathematical Tables* (Dover, New York, 1970).
[56] F. H. Claro and G. H. Wannier, Phys. Rev. B **19**, 6068 (1979).
[57] Y. Hatsugai and M. Kohmoto, Phys. Rev. B **42**, 8282 (1990).
[58] D. J. Thouless, Phys. Rev. B **28**, 4272 (1983).
[59] J. H. Han, D. J. Thouless, H. Hiramoto, and M. Kohmoto, Phys. Rev. B **50**, 11365 (1994).
[60] D. J. Thouless, Phys. Rep. **13**, 93 (1974); J. T. Edwards and D. J. Thouless, J. Phys. C: Solid State Phys. **4**, 453 (1971).
[61] R. J. Bell and P. Dean, Discuss. Faraday Soc. **50**, 55 (1970).
[62] F. Liu, S. Ghosh, and Y. D. Chong, Phys. Rev. B **91**, 014108 (2015).
[63] J. B. Sokoloff, Phys. Rep. **126**, 189 (1985).
[64] A. Janner and T. Janssen, Phys. Rev. B **15**, 643 (1977).